

NUMERICAL CONVERGENCE OF NONLINEAR NONLOCAL CONTINUUM MODELS TO LOCAL ELASTODYNAMICS*

PRASHANT K. JHA [†] AND ROBERT LIPTON [‡]

Abstract. We investigate the error incurred in replacing a nonlinear nonlocal bond based peridynamic model with linearized peridynamics or classic local elastodynamics away from the fracture set. The nonlinear nonlocal model is characterized by a double well potential. We establish a convergence rate for differentiable solutions of nonlinear nonlocal peridynamics to the solution of classical linear elastodynamics. The convergence rate is shown to be linear in the length scale of non locality and uniform in time. The linear rate also holds for the convergence of solutions of the linearized peridynamic model to the classical elastodynamics solution. The consistency error of numerical approximation for peridynamics is shown to explicitly depend on the ratio of mesh size and peridynamic horizon. For central difference schemes in time and linear interpolation in space the stability condition for linearized peridynamics is shown to be given by a generalization of the CFL condition. Numerical results are presented to illustrate how nonlinear and linearized peridynamics converge to classical elastodynamics.

Key words. Peridynamic modeling, numerical analysis, finite element approximation, nonlocal mechanics

AMS subject classifications. 34B10, 74H55, 74S20

1. Introduction. The nonlocal formulation proposed in [28] provides a framework for modeling crack propagation inside solids. The basic idea is to redefine the strain in terms of the difference quotients of the displacement field and allow for nonlocal forces acting within some finite horizon. The relative size of the horizon with respect to the diameter of the material domain is denoted by ϵ . The force at any given material point is determined by the deformation of all neighboring material points surrounding it within a radius given by the size of horizon. Earlier work, in the absence of fracture, demonstrates the convergence of linear nonlocal peridynamic models to local model of linear elasticity, see [37], [30]. The convergence of a peridynamic model to the Navier equation in the sense of solution operators is established in [26]. Computational fracture modeling using peridynamics feature formation and evolution of interfaces associated with fracture is discussed in [27], [6], [19], [2], [17], [11], [7], [10], [16], [20], [31], [27], [35], [29], and [24]. Theoretical analysis of different mechanical and mathematical aspects of peridynamic models can be found in [16], [25], [13], [14], [4], and [3]. A theory of dynamic phase transformation has been introduced in the context of peridynamic theory in [10]. Recently in [9] the nonlocality in kinetic energy, as a complement to the nonlocal elastic energy for consistent energetics and dynamics, is discussed. A full accounting of the peridynamics literature lies beyond the scope of this paper however several themes and applications are covered in the recent hand book [15].

In this work we examine the discrete approximations to the nonlinear nonlocal model developed in [22], [23]. One of the important and rigorously established points of this peridynamic model is the fact that as the size of the horizon goes to zero, i.e. when we tend to the local limit, the solution of this model converges to an evolving displacement - crack set pair where the displacement evolves according to the elastic wave equation away from the crack set and the complete evolution described by fracture and displacement has

*Article submitted for review in International Journal for Numerical Methods in Engineering on July 1, 2017.

Funding: This material is based upon work supported by the Army Research Office under award W911NF-16-1-0456.

[†]Department of Mathematics, Louisiana State University, Baton Rouge, LA (prashant.j16o@gmail.com).

[‡]Department of Mathematics, Louisiana State University, Baton Rouge, LA (lipton@math.lsu.edu).

bounded Griffith fracture energy. To clearly present and illustrate the ideas we will work with the one-dimensional version of the nonlocal model.

In this paper we are motivated by adaptive implementations of peridynamic models for brittle fracture. In regions of the body where there is no fracture we would like to model the material as linear elastic while in regions where fracture is anticipated we would use the nonlinear nonlocal peridynamics model [22], [23]. With this in mind we investigate the difference between numerically computed solutions for the nonlinear nonlocal bond based model with those of the linearized nonlocal model, and those of classic local elastodynamics. We assume a-priori knowledge on the differentiability of the solution of our nonlinear peridynamic model. Subject to this assumption we find that the solutions of the nonlinear model converge to classical elastodynamics at a rate that is linear in ϵ . We analyze the numerical approximation associated with linear interpolation in space for two cases: i.) when the size of horizon is fixed and the mesh size h tends to zero, known as h -convergence, and ii.) when the size of the horizon also tends to zero with the mesh, known in the literature as m -convergence. For the first case we show consistency error is of order $O(\frac{h}{\epsilon})$ for both nonlinear and linearized models, see [Proposition 4](#). For the second we find that the consistency error for both models is $O(\frac{h}{\epsilon}) + O(\epsilon)$, see [Proposition 5](#). Stability for the central difference in time approximation to the linearized model is given by a modified CFL condition, see [Theorem 6](#). Earlier work [21] analyzed the same model but for more general initial data that generated non differentiable Hölder continuous solutions. For that case solutions can approach discontinuous deformations (fracture like solutions) and it is shown that the numerical approximation of the nonlinear model in dimension $d = 1, 2, 3$ converges to the exact solution at the rate $O(\Delta t + h^\gamma/\epsilon^2)$ where $\gamma \in (0, 1]$ is the Hölder exponent, h is the size of mesh, ϵ is the size of horizon, and Δt is the size of time step. The work presented here shows that we can improve the rate of convergence for this model if we have a-priori knowledge on the number of bounded continuous derivatives of the solution.

We point out that earlier numerical analysis of linear peridynamic models for 1-d bars have been given in [37] and [7]. Meshfree approximation methods are discussed in [29]. Related approximations of nonlocal diffusion models are discussed in [33], [8], and [12]. In [18], the stability of the numerical approximation to solutions of linear nonlocal wave equations are discussed in detail.

Solutions of nonlocal models exhibit wave dispersion whereas solutions to linear local elastodynamics do not. For certain peridynamic models this aspect is analyzed in [38] and [36]. Recently in [5] wave dispersion is discussed in detail for the bond based and state based models. In [section 5](#), we pursue this and present wave dispersion plot for different choices of influence function. We find that the wave dispersion is strong when the nonlocal effect is significant, i.e., for larger horizon and bond forces. Whereas the dispersive effect decreases when size of horizon is small relative to the computational domain. We show that the peridynamic solution approaches the solution of local elastodynamics and the wave dispersion vanishes as the horizon goes to zero. On the other hand, for both nonlinear and linear nonlocal models, the consistency error decreases as $O(\frac{h}{\epsilon}) + O(\epsilon)$. This is also confirmed by our numerical experiments which show that the error due to discretization can be minimized by choosing the ratio h/ϵ suitably small for every choice of ϵ as $\epsilon \rightarrow 0$, see [Figure 6](#). Our results are consistent with asymptotically compatible schemes developed for linear stationary nonlocal models in [32], [33], [34]. We verify convergence rates by integrating the peridynamic model long enough to include the boundary effects due to wave reflection in [subsection 6.1](#). Our numerical studies confirm that the solutions of linear and nonlinear peridynamics are indistinguishable for sufficiently small horizon ϵ when a-priori regularity is assumed.

The results of this analysis rigorously show that one can use a discrete linear local elas-

todynamic model to approximate the nonlinear nonlocal evolution when sufficient regularity of the evolution is known a-priori. In doing so one incurs a modeling error of order ϵ but saves computational work in that there is no nonlocality so the mesh diameter h no longer has to be small relative to ϵ . The discretization error is now associated with the approximation error for the initial boundary value problem for the linear elastic wave equation. We close the introduction noting that recent adaptive approaches to mesh generation for nonlocal problems are presented in [39], [35], [6].

The organization of this article is as follows: In [section 2](#), we introduce the class of nonlocal nonlinear potentials and state the convergence of the associated evolution to that of linear local elastodynamics when it is known a-priori that the solutions are sufficiently smooth. In [section 3](#), we discuss the finite element approximation of the model and show the bound on consistency error due to discretization. In [section 4](#), we consider the central time difference scheme and obtain a stability condition on Δt as function of ϵ and h . Wave dispersion in the nonlocal model is analyzed in [section 5](#). In [section 6](#), we present the results of numerical simulation. The proofs of the theorems are given in [section 7](#). We conclude in [section 8](#).

2. Nonlocal evolution and elastodynamics. Let $D := [a, b] \subset \mathbb{R}$ be a bounded material domain in one dimension and $J = [0, T]$ be an interval of time. The nonlocal boundary denoted by ∂D^ϵ are intervals of diameter 2ϵ on either side of D and given by $(a - 2\epsilon, a) \cup (b, b + 2\epsilon)$. The strain S for the one dimensional peridynamic model is given by the difference quotient

$$S(y, x; u) := \frac{u(y) - u(x)}{|y - x|}.$$

The nonlocal force is given in terms of the non-linear two-point interaction potential W^ϵ defined by

$$W^\epsilon(S, y - x) = \frac{2J^\epsilon(|y - x|)}{\epsilon |y - x|} f(|y - x| S^2),$$

where $f : \mathbb{R}^+ \rightarrow \mathbb{R}$ is assumed to be positive, smooth, and concave with following properties

$$(1) \quad \lim_{r \rightarrow 0^+} \frac{f(r)}{r} = f'(0), \quad \lim_{r \rightarrow \infty} f(r) = f_\infty < \infty.$$

The potential $W^\epsilon(S, y - x)$ is of double well type and convex near the origin where it has one well and concave and bounded at infinity where it has the second well associated with the horizontal asymptote $W^\epsilon(\infty, y - x)$, see [Figure 1](#). The function $J^\epsilon(|y - x|)$ influences the magnitude of the nonlocal force due to y on x . We define J^ϵ by rescaling $J(|\xi|)$, i.e. $J^\epsilon(|\xi|) = J(|\xi|/\epsilon)$. The influence function J is zero outside the ball $[-1, 1]$, and satisfies $0 \leq J(|\xi|) \leq M$ for all $\xi \in [-1, 1]$.

The force of two point interaction between x and y is derived from the nonlocal potential and given by $\partial_S W^\epsilon(S, y - x)$, see [Figure 2](#). For small strains the force is linear and elastic and then softens as the strain becomes larger. The critical strain, for which the force between x and y begins to soften, is given by $S_c(y, x) := \bar{r}/\sqrt{|y - x|}$ and the force decreases monotonically for

$$|S(y, x; u)| > S_c.$$

Here \bar{r} is the inflection point of $r \rightarrow f(r^2)$, and is the root of following equation

$$f'(r^2) + 2r^2 f''(r^2) = 0.$$

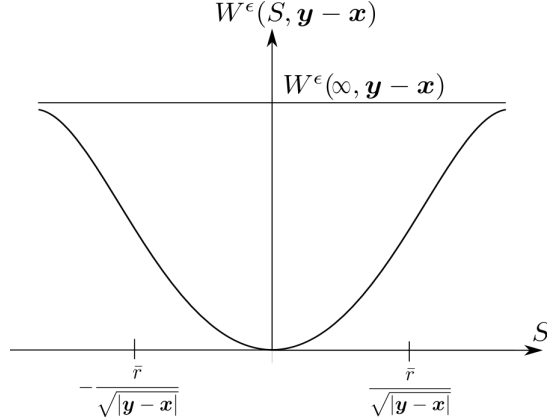


Fig. 1: Two-point potential $W^\epsilon(S, y - x)$ as a function of strain S for fixed $y - x$.

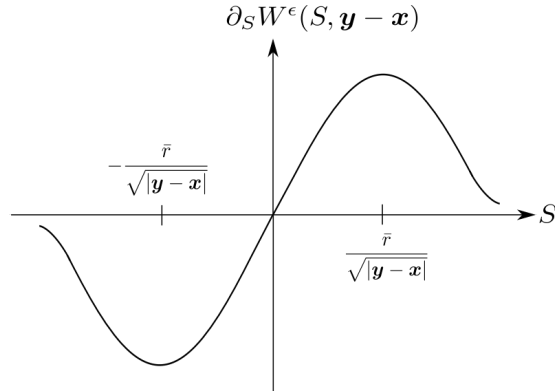


Fig. 2: Nonlocal force $\partial_S W^\epsilon(S, y - x)$ as a function of strain S for fixed $y - x$. Second derivative of $W^\epsilon(S, y - x)$ is zero for $S = S_c := \pm \bar{r} / \sqrt{|y - x|}$.

The nonlocal force $-\nabla PD^\epsilon$ is defined by

$$\begin{aligned} -\nabla PD^\epsilon(u)(x) &= \frac{1}{2\epsilon} \int_{x-\epsilon}^{x+\epsilon} \partial_S W^\epsilon(S, y - x) dy \\ &= \frac{2}{\epsilon^2} \int_{x-\epsilon}^{x+\epsilon} J(|y - x|/\epsilon) f'(|y - x|) S(y, x; u)^2 S(y, x; u) dy. \end{aligned}$$

Similarly, we denote $-\nabla PD_l^\epsilon(u)(x)$ as the linearized peridynamic force at x , given by

$$-\nabla PD_l^\epsilon(u)(x) = \frac{2}{\epsilon^2} \int_{x-\epsilon}^{x+\epsilon} J(|y - x|/\epsilon) f'(0) S(y, x; u)^2 S(y, x; u) dy.$$

The corresponding linear local model is characterized by the Young's modulus \mathbb{C} given by

$$(2) \quad \begin{aligned} \mathbb{C} &= \int_{-1}^1 J(|z|) f'(0) |z| dz \\ &= \frac{1}{\epsilon^2} \int_{x-\epsilon}^{x+\epsilon} J(|y-x|/\epsilon) f'(0) |y-x| dy, \quad \forall x, \epsilon > 0. \end{aligned}$$

Let u^ϵ be the solution of the peridynamic equation of evolution, u_l^ϵ be the solution of the linearized peridynamic equation of evolution, and u be the solution of elastodynamic equation of evolution with Young's modulus \mathbb{C} . For comparison of u_l^ϵ and u^ϵ with u , we assume u to be extended to $D \cup \partial D^\epsilon$ by zero outside D . The displacements u^ϵ , u_l^ϵ , and u satisfy following evolution equations, for all $(x, t) \in D \times J$, described by

$$(3) \quad \rho \ddot{u}(t, x) = \mathbb{C} u_{xx}(t, x) + b(t, x),$$

$$(4) \quad \rho \ddot{u}^\epsilon(t, x) = -\nabla P D^\epsilon(u^\epsilon(t))(x) + b(t, x),$$

$$(5) \quad \rho \ddot{u}_l^\epsilon(t, x) = -\nabla P D_l^\epsilon(u_l^\epsilon(t))(x) + b(t, x),$$

where $b(t, x)$ is a prescribed body force and the mass density ρ is taken to be constant. The boundary conditions are given by

$$u^\epsilon(t, x) = 0 \quad \text{and} \quad \dot{u}^\epsilon(t, x) = 0, \quad \forall t \in J, \forall x \in \partial D^\epsilon,$$

and the same boundary conditions hold for u_l^ϵ and u . The initial condition is given by

$$u^\epsilon(0, x) = g(x) \quad \text{and} \quad \dot{u}^\epsilon(0, x) = h(x), \quad \forall x \in D,$$

and the same initial condition also hold for u_l^ϵ and u .

Before we proceed with the numerical analysis, we first show that the solution u^ϵ of peridynamic equation converges, in the limit $\epsilon \rightarrow 0$, to the solution u of the elastodynamic equation. In what follows $C^n(D)$ is the space of functions with n continuous derivatives on D .

PROPOSITION 1 (Control on the difference between peridynamic force and elastic force).
If $u \in C^3(D)$, and

$$\sup_{(x) \in D} |u_{xxx}(x)| < \infty,$$

then

$$(6) \quad \sup_{x \in D} |-\nabla P D^\epsilon(u)(x) - (-\nabla P D_l^\epsilon(u)(x))| = O(\epsilon),$$

$$(7) \quad \sup_{x \in D} |-\nabla P D_l^\epsilon(u)(x) - \mathbb{C} u_{xx}(x)| = O(\epsilon),$$

so

$$(8) \quad \sup_{x \in D} |-\nabla P D^\epsilon(u)(x) - \mathbb{C} u_{xx}(x)| = O(\epsilon).$$

If $u \in C^4(D)$, and

$$(9) \quad \sup_{(x) \in D} |u_{xxxx}(x)| < \infty,$$

then

$$(10) \quad \sup_{x \in D} |-\nabla P D_l^\epsilon(u)(x) - \mathbb{C} u_{xx}(x)| = O(\epsilon^2).$$

We now state the theorem which shows that $u^\epsilon \rightarrow u$ with rate ϵ in the $H^1(D)$ norm uniformly in time.

THEOREM 2 (Convergence of nonlinear peridynamics to the linear elastic wave equation in the limit that the horizon goes to zero). *Let $e^\epsilon := u^\epsilon - u$, where u^ϵ is the solution of Equation 4 and u is the solution of Equation 3. Suppose $u^\epsilon(t) \in C^4(D)$, for all $\epsilon > 0$ and $t \in [0, T]$. Suppose there exists $C_1 > 0$, C_1 independent of the size of horizon ϵ , such that*

$$\sup_{\epsilon > 0} \left[\sup_{(x,t) \in D \times J} |u_{xxxx}^\epsilon(t,x)| \right] < C_1 < \infty.$$

Then, $\exists C_2 > 0$ such that

$$\sup_{t \in [0, T]} \left\{ \int_D \rho |\dot{e}^\epsilon(t, x)|^2 dx + \int_D \mathbb{C} |e_x^\epsilon(t, x)|^2 dx \right\} \leq C_2 \epsilon^2$$

so $u^\epsilon \rightarrow u$ in the $H^1(D)$ norm at the rate ϵ uniformly in time $t \in [0, T]$.

A stronger convergence result holds for the solutions $u_l^\epsilon(t)$ of the family of linearized peridynamic equations.

THEOREM 3 (Convergence of linearized peridynamics equation to the linear elastic wave equation in the limit that the horizon goes to zero). *Let $e_l^\epsilon := u_l^\epsilon - u$, where u_l^ϵ is the solution of Equation 5 and u is the solution of Equation 3. Suppose $u_l^\epsilon(t) \in C^4(D)$, for all $\epsilon > 0$ and $t \in [0, T]$. Suppose there exists $C_1 > 0$, C_1 independent of the size of horizon ϵ , such that*

$$\sup_{\epsilon > 0} \left[\sup_{(x,t) \in D \times J} |(u_l^\epsilon)_{xxxx}(t,x)| \right] < C_1 < \infty.$$

Then, $\exists C_2 > 0$ such that

$$\sup_{t \in [0, T]} \left\{ \int_D \rho |\dot{e}_l^\epsilon(t, x)|^2 dx + \int_D \mathbb{C} |(e_l^\epsilon)_x(t, x)|^2 dx \right\} \leq C_2 \epsilon^4$$

so $u_l^\epsilon \rightarrow u$ in the $H^1(D)$ norm at the rate ϵ^2 uniformly in time $t \in [0, T]$.

The proofs of Proposition 1, Theorem 2 and Theorem 3 is postponed to section 7. We now discuss the finite element approximation of the peridynamic model and show the consistency of the discretization for both piecewise constant and linear interpolation.

3. Finite element approximation. We first discretize the peridynamic equation in space. In the following section 4 we will discretize in time and investigate the stability of the central difference scheme. Let h be the size of mesh given by the distance between grid points and let \overline{D} and $\overline{\partial D^\epsilon}$ denote the closure of the sets D and ∂D^ϵ . We suppose \overline{D} and $\overline{\partial D^\epsilon}$ contain an integral number of elements of the mesh. Let $D_h = D \cap h\mathbb{Z}$ and $\partial D^{\epsilon, h} = \partial D^\epsilon \cap h\mathbb{Z}$, and let $K = \{i \in \mathbb{Z} : ih \in \overline{D}\}$ and $K_\epsilon = \{i \in \mathbb{Z} : ih \in \overline{\partial D^\epsilon}\}$. Here K_ϵ corresponds to the list of nodes located inside the closure of the nonlocal boundary ∂D^ϵ . We assume $x_i = ih$. We define the interpolation operator $I_h[\cdot]$, for a given function $g : \overline{D \cup \partial D^\epsilon} \rightarrow \mathbb{R}$ as follows

$$\mathcal{I}_h[g(y)] = \sum_{i \in K \cup K_\epsilon} g(x_i) \phi_i(y),$$

where $\phi_i(\cdot)$ is the interpolation function associated to the node i and $\{\phi_i\}_{i \in K \cup K_\epsilon}$ is a partition of unity, i.e.,

$$\sum_{i \in K \cup K_\epsilon} \phi_i(x) = 1$$

for all $x \in \overline{D \cup \partial D^\epsilon}$. In order to expedite the presentation we assume the diameter of nonlocal interaction 2ϵ is fixed and always contains an integral number of grid points $2m+1$. For this choice $\epsilon = mh$ where m increases as h decreases. When we investigate m convergence we will allow both ϵ and h to decrease.

We also consider extensions of discrete sets defined on the nodes $K \cup K_\epsilon$. We write the function $v(t, x_i)$ defined at node x_i as $v_i(t)$ and define the discrete set $\{v_i(t)\}_{K \cup K_\epsilon}$. The function $\hat{u}_h^\epsilon(t)$ is the extension of discrete set $\{\hat{u}_i^\epsilon(t)\}_{K \cup K_\epsilon}$ using the interpolation functions and is defined by

$$\hat{u}_h^\epsilon(t) = E[\{\hat{u}_i^\epsilon(t)\}_{K \cup K_\epsilon}] = \sum_{i \in K \cup K_\epsilon} \hat{u}_i^\epsilon(t) \phi_i(x), \quad \forall x \in \overline{D \cup \partial D^\epsilon}.$$

We also have the body force $b_h(t)$ given by the extension of discrete set $\{b_i(t)\}_{K \cup K_\epsilon}$ defined by

$$b_h(t) = E[b_i(t)]_{K \cup K_\epsilon} = \sum_{i \in K \cup K_\epsilon} b_i(t) \phi_i(x), \quad \forall x \in \overline{D \cup \partial D^\epsilon}.$$

Let $\hat{u}_h^\epsilon(t)$ be the solution of following equation

$$(11) \quad \rho \ddot{\hat{u}}_h^\epsilon(t) = -\nabla P D^\epsilon(\hat{u}_h^\epsilon(t))(x_i) + b_i(t),$$

with initial condition defined at the nodes given by

$$\hat{u}_i^\epsilon(0) = f(x_i), \quad \dot{\hat{u}}_i^\epsilon(0) = g(x_i), \quad \forall i \in K,$$

or equivalently given by the extension of the discrete sets

$$(12) \quad \hat{u}_h^\epsilon(0) = f_h, \quad \dot{\hat{u}}_h^\epsilon(0) = g_h, \quad \forall i \in K,$$

and homogeneous boundary condition given by

$$(13) \quad \hat{u}_i^\epsilon(t) = 0, \quad \dot{\hat{u}}_i^\epsilon(t) = 0, \quad \forall i \in K_\epsilon.$$

Similarly, the discrete set $\{\hat{u}_{l,i}^\epsilon(t)\}_{i \in K \cup K_\epsilon}$, with subscript l , is extended by interpolation to the function $\hat{u}_{l,h}^\epsilon(t) = E[\{\hat{u}_{l,i}^\epsilon(t)\}_{i \in K \cup K_\epsilon}]$ and satisfies the linear peridynamic equation

$$(14) \quad \begin{aligned} \rho \ddot{\hat{u}}_{l,i}^\epsilon(t) &= -\nabla P D^\epsilon(\hat{u}_{l,h}^\epsilon(t))(x_i) + b_i(t) \\ &= \frac{2}{\epsilon^2} \sum_{\substack{j \in K \cup K_\epsilon, \\ j \neq i}} f'(0)(\hat{u}_{l,j}^\epsilon(t) - \hat{u}_{l,i}^\epsilon(t)) \int_{x_i - \epsilon}^{x_i + \epsilon} \frac{\phi_j(y) J(|y - x_i|/\epsilon)}{|y - x_i|} dy + b_i(t), \end{aligned}$$

with initial conditions [Equation 12](#) and boundary conditions [Equation 13](#). The evolution equation for a discrete approximation to the linearized peridynamic equation can be written in a compact vector form. Let $U_{l,h}(t) = (\hat{u}_{l,i}^\epsilon(t))_{i \in K}$ be the vector of the approximate solution evaluated at the nodes. Then, we can write the [Equation 14](#) in the matrix form

$$(15) \quad \rho \ddot{U}_{l,h}(t) = A U_{l,h}(t) + B(t),$$

where a_{ij} are defined as

$$(16) \quad a_{ij} = \begin{cases} \bar{a}_{ij} & \text{if } j \neq i, \\ -\sum_{k \in K \cup K_\epsilon, k \neq i} \bar{a}_{ik} & \text{if } j = i \end{cases}$$

where

$$(17) \quad \bar{a}_{ij} = \frac{2}{\epsilon^2} f'(0) \int_{x_i - \epsilon}^{x_i + \epsilon} \frac{\phi_j(y) J(|y - x_i|/\epsilon)}{|y - x_i|} dy.$$

$B(t) = (b_i(t))_{i \in K}$ is the body force vector with

$$b_i(t) = b(t, x_i).$$

We mention that nonzero nonlocal boundary conditions can be prescribed on ∂D^ϵ . For this case we include the known displacement corresponding to the nonlocal boundary K_ϵ by incorporating these boundary displacements on the right hand side vector as is given below,

$$b_i(t) = b(t, x_i) + \sum_{j \in K_\epsilon, j \neq i} \bar{a}_{ij} \hat{u}_{l,j}^\epsilon.$$

In this paper we use linear continuous interpolation functions $\phi_i(x)$.

Linear continuous interpolation: Let $i \in K \cup K_\epsilon$. We define $\phi_i(x)$ as follows

$$\phi_i(x) = \begin{cases} 0 & \text{if } x \notin [x_{i-1}, x_{i+1}], \\ \frac{x - x_{i-1}}{h} & \text{if } x \in [x_{i-1}, x_i], \\ \frac{x_{i+1} - x}{h} & \text{if } x \in [x_i, x_{i+1}], \end{cases}$$

with $x_{i+1} - x_i = h$, $i \in K \cup K_\epsilon$ and

$$\sum_{i \in K \cup K_\epsilon} \phi_i = 1,$$

and for $g \in C^2(\overline{D})$ we have

$$|\mathcal{I}_h[g(x)] - g(x)| \leq \sup_z |g''(z)|h^2.$$

3.1. Consistency error. In this section, we present upper bounds on the consistency error due to the quadrature based finite element discretization for both the nonlinear non-local peridynamic force and the linearized nonlocal peridynamic force.

h -convergence: We keep ϵ fixed and estimate the error with respect to mesh size h characterized the distance between interpolation points h .

PROPOSITION 4 (Consistency error: peridynamic approximation). *For linear continuous interpolation, if $u \in C^3(D)$ and u_{xxx} is bounded on D then we have for linearized peridynamic force*

$$(18) \quad \sup_{i \in K} |\nabla \text{PD}_l^\epsilon(\mathcal{I}_h[u])(x_i) - \nabla \text{PD}_l^\epsilon(u)(x_i)| = O(h/\epsilon),$$

and for the nonlinear peridynamic force

$$(19) \quad \sup_{i \in K} |\nabla \text{PD}^\epsilon(\mathcal{I}_h[u])(x_i) - \nabla \text{PD}^\epsilon(u)(x_i)| = O(h/\epsilon).$$

m -convergence: In this case, we let ϵ to zero as well as h with $\epsilon > h$. Combining Proposition 1, Proposition 4 and applying the triangle inequality gives:

PROPOSITION 5 (Consistency error: peridynamic approximation in the limit $\epsilon \rightarrow 0$). *For linear continuous interpolation, if $u \in C^3(D)$ with u_{xxx} bounded then we have for the linearized peridynamic force*

$$(20) \quad \sup_{i \in K} | -\nabla PD_l^\epsilon(\mathcal{I}_h[u])(x_i) - \mathbb{C}u_{xx}(x_i) | = O(\epsilon) + O(h/\epsilon),$$

and for the nonlinear peridynamic force

$$(21) \quad \sup_{i \in K} | -\nabla PD^\epsilon(\mathcal{I}_h[u])(x_i) - \mathbb{C}u_{xx}(x_i) | = O(\epsilon) + O(h/\epsilon).$$

This Proposition shows that the consistency error for both nonlinear and linearized nonlocal models is controlled by the ratio of the mesh size to the horizon. This ratio must decrease to zero as the horizon goes to zero in order for the consistency error to go to zero.

4. Central difference scheme and stability analysis. In this section, we consider the central difference time discretization of semi-discrete peridynamic equation [Equation 11](#). We obtain the stability condition for the linearized peridynamic equation. Under certain conditions this can imply the stability of nonlinear peridynamic solution. This can happen if the acceleration and body force are sufficiently small; in this scenario one can approximate the nonlinear peridynamics by its linearization. Let Δt be the time step and the field $u(t)$ at time step $k\Delta t$ is denoted by u^k . To illustrate ideas we will assume $\rho = 1$. For the linearized peridynamics we characterize the matrix A associated with the spatial discretization [Equation 15](#). We introduce a special class of matrices.

Definition. An M-matrix has negative off diagonal elements m_{ij} , $i \neq j$, and the diagonal elements satisfy $m_{ii} \geq \sum_{j \neq i} m_{ij}$ for all i .

The stability of the numerical scheme is based on the following property of A .

LEMMA 1 (Properties of the A matrix). *For linear interpolations, the square matrix $-A$ of size $|K| \times |K|$ is a Stieltjes matrix, i.e. it is a nonsingular symmetric M-matrix. Therefore, the eigenvalues of $-A$ are real and positive.*

Proof. $-A$ is clearly M-matrix as its off-diagonal terms are negative, and diagonal terms satisfy $-a_{ii} \geq \sum_{j \neq i} -a_{ij}$ for all i . To prove that a M matrix is nonsingular, we apply Theorem 2.3 in [\[1\]](#), Chapter 6]. From the definition of $-A$ we find that

$$-a_{ii} = \sum_{i \neq j} -a_{ij}, \quad i = 1, \dots, n, \quad -a_{ii} > \sum_{j=1}^{i-1} -a_{ij}, \quad i = 2, \dots, n,$$

and this is easily seen to be condition M_{37} of Theorem 2.3 and we conclude that $-A$ is nonsingular. The symmetry of $-A$ is a straight forward consequence of the formula [Equation 17](#). \square

Central difference time discretization: For $\rho = 1$, the spatially discretized evolution equations for linearized peridynamics given by [Equation 15](#) is written

$$\ddot{U}_{l,h}(t) = AU_{l,h}(t) + B(t).$$

We now additionally discretize in time using the central difference scheme. Let $U_{l,h}^k := \{\dot{u}_{l,i}^{\epsilon,k}\}_{i \in K}$ denote the discrete displacement field at time step k . Here we use the subscript “ l ” for linear peridynamic and superscript “ ϵ ” to highlight that the solution corresponds to size of horizon ϵ . In what follows, we will assume no body force and the dynamics is driven by the initial conditions. Since we have the zero Dirichlet boundary condition, we know

the displacement at nodes $i \in K_\epsilon$ is zero for all time steps. We assume $k \leq T/\Delta t$, and the horizon is given by $\epsilon = mh/2$ where m is a positive integer. The discretized dynamics is given by the solution $\{U_{l,h}^k\}$ of the following equation

$$\frac{U_{l,h}^{k+1} - 2U_{l,h}^k + U_{l,h}^{k-1}}{\Delta t^2} = AU_{l,h}^k,$$

or after elementary manipulation

$$(22) \quad U_{l,h}^{k+1} = -U_{l,h}^{k-1} + (2 + \Delta t^2 A)U_{l,h}^k.$$

THEOREM 6 (Stability criterion for the central difference scheme). *Recall the elastic constant \mathbb{C} given by Equation 2, $f'(0)$ given by Equation 1, and $M = \max_{0 < r \leq 1} \{J(r)\}$. Then the central difference scheme Equation 22, in the absence of body forces, is stable as long as Δt satisfies*

$$(23) \quad \Delta t \leq \frac{h}{\sqrt{\mathbb{C} + 2f'(0) \frac{Mh^2}{\epsilon^2}}}.$$

Remark. The stability condition for the linear elastic wave equation is given by the CFL condition $\Delta t \leq \frac{h}{\sqrt{\mathbb{C}}}$ where h gives the distance between mesh points.

Proof. Let $(\gamma_i, \boldsymbol{\nu}_i)$ be an eigenpair of A . Let $\lambda_i = -\gamma_i$, then $\lambda_i > 0$ and let $\lambda = \max_i \{\lambda_i\}$. Substitute $U_{l,h}^k = \xi^k \boldsymbol{\nu}$, where ξ is some real number and by ξ^k we mean the k^{th} power of ξ , into Equation 22, to obtain the characteristic equation

$$\xi^2 - 2\theta\xi + 1 = 0.$$

where $\theta = 1 - 1/2\lambda_i\Delta t^2$. The solution of the quadratic equation gives two roots: $\delta_1 = \theta + \sqrt{\theta^2 - 1}$ and $\delta_2 = \theta - \sqrt{\theta^2 - 1}$. We need $|\delta| \leq 1$ for stability. Since $\delta_1\delta_2 = 1$, the only possibility is when $|\delta_1| = |\delta_2| = 1$. This is satisfied for all eigenmodes when

$$\begin{aligned} |\theta| &\leq 1 \\ \Rightarrow \Delta t &\leq \frac{2}{\sqrt{\lambda}} \leq \frac{2}{\sqrt{\lambda_i}}. \end{aligned}$$

A lower estimate on $1/\sqrt{\lambda}$ follows from Gershgorin's circle theorem:

THEOREM 7. *Any eigenvalue of A lies inside at least one of the disks*

$$(24) \quad |\gamma - a_{ii}| < \sum_{i \neq j} |a_{ij}|.$$

All eigenvalues of A lie on the negative real axis and we provide an upper estimate on the largest magnitude of the eigenvalues depending only on the mesh size h given by the distance between interpolation points and the horizon $\epsilon = mh$. For this case, it follows from Equation Equation 24 and Equation 16 that

$$\lambda < 2 \sum_{i \neq j} \bar{a}_{ij},$$

Writing out the sum and using the definition of the interpolating functions and their partition of unity properties we get

$$\begin{aligned} \sum_{i \neq j} \bar{a}_{ij} &= \frac{2f'(0)}{\epsilon^2} \int_{x_{i-1}}^{x_{i+1}} \frac{1}{h} J(|y - x_i|/\epsilon) dy \\ &+ \frac{2f'(0)}{\epsilon^2} \int_{x_i - \epsilon}^{x_{i-1}} \frac{J(|y - x_i|/\epsilon)}{|y - x_i|} dy \\ &+ \frac{2f'(0)}{\epsilon^2} \int_{x_{i+1}}^{x_i + \epsilon} \frac{J(|y - x_i|/\epsilon)}{|y - x_i|} dy. \end{aligned}$$

Here we make use of the identities

$$\begin{aligned} 1 &= \sum_{j \in I^+} \phi^j(y), y \in [x_{i+1}, x_i + \epsilon], \\ 1 &= \sum_{j \in I^-} \phi^j(y), y \in [x_i - \epsilon, x_{i-1}], \end{aligned}$$

where $I^+ = \{j : x_j \in [x_{i+1}, x_i + \epsilon]\}$ and $I^- = \{j : x_j \in [x_i - \epsilon, x_{i-1}]\}$. For $y < x_{i-1}$ and $x_{i+1} < y$ we have $h < |y - x_i|$ and $1 < |y - x_i|/h$ and we have the estimate

$$\begin{aligned} \sum_{i \neq j} \bar{a}_{ij} &\leq 2 \frac{\mathbb{C}}{h^2} + \frac{2f'(0)}{h\epsilon^2} \int_{x_{i-1}}^{x_{i+1}} J(|y - x_i|/\epsilon) dy \\ &\leq 2 \frac{\mathbb{C}}{h^2} + \frac{4}{\epsilon^2} f'(0) M, \end{aligned}$$

and a lower bound now follows on $1/\sqrt{\lambda}$. Simple manipulation then delivers [Equation 23](#). \square

5. Wave dispersion in peridynamic models. Consider a single wave $u(t, x) = a \cos(\kappa(x - \nu t))$ with the wave number κ . For the linear elastic model, the phase velocity will be constant, and is given by $\nu = \sqrt{\mathbb{C}/\rho}$, where \mathbb{C} is the elasticity constant. This is not the case in nonlocal models. With u described as above, strain is given by

$$S(y, x) = \frac{u(x, t)}{|y - x|} [(\cos(\kappa(y - x)) - 1) + (-\tan(\kappa(x - \nu t)) \sin(\kappa(y - x)))].$$

Substituting this in the finite element approximation [Equation 11](#) to get the following nonlinear equation for phase velocity

$$\begin{aligned} \nu^2 &= \frac{2}{\epsilon^2 \kappa^2} \sum_{j=-\epsilon/h-1, j \neq 0}^{\epsilon/h+1} \bar{a}_{0j} f'(|j| h S(jh, 0)^2) \left[\left(\frac{1 - \cos(\kappa(y - x))}{|j| h} \right) \right. \\ &\quad \left. + \left(-\frac{\tan(\kappa(x - \nu t)) \sin(\kappa(y - x))}{|j| h} \right) \right]. \end{aligned}$$

In case of linear peridynamics, we factor out $f'(0)$, and cancel the odd term with $\sin(\kappa(y - x))$, to get

$$\nu^2 = -\frac{4f'(0)}{\epsilon^2 \kappa^2} \sum_{j=1}^{\epsilon/h+1} \bar{a}_{0j} \frac{1 - \cos(\kappa j h)}{jh}.$$

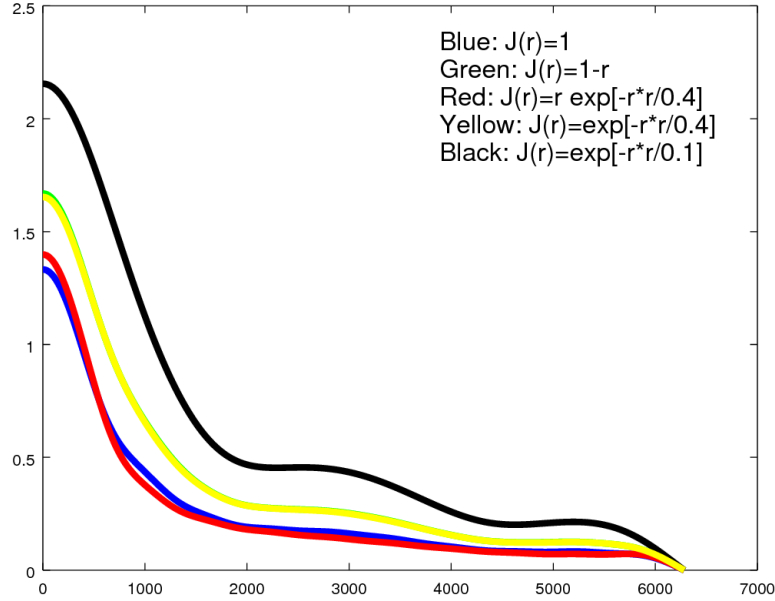


Fig. 3: Normalized phase velocity ν/\sqrt{C} vs wave number κ for different influence functions $J(r)$.

Recall that \bar{a}_{ij} is defined in [Equation 17](#). Since $\bar{a}_{0j} = \bar{a}_{0(-j)}$, and $\bar{a}_{0j} \geq 0$ for all j , we conclude that ν is real and positive for each κ . [Figure 3](#) shows ν vs κ plot for different influence functions.

One interesting point to note is that for the influence function $J(r) = \exp[-r^2/\beta]$, we see that if the decay rate in the influence function, with respect to bond length, increases then the phase velocity is also increases. [Figure 4](#) shows the trend in the dispersion curves as we let $\epsilon \rightarrow 0$. It is clear that dispersion vanishes as the nonlocal interaction tends to zero.

6. Numerical simulation. In this section, we present the results of numerical simulation. We start by writing down the nondimensional dynamics in [subsection 6.1](#). We then do a numerical study of the h -convergence in [subsection 6.2](#) and the m -convergence in [subsection 6.3](#). We compare the numerical simulations for the nonlinear and linear nonlocal models with the local linear elastodynamics.

6.1. Nondimensional peridynamic equation. Let $[0, L]$ be the bar with length L in meters. Let $[0, T]$ be the time domain in units of seconds. Given a dimensionless influence function $J(r), r \in [0, 1]$, the bond force $f'(0)$ is in the units N/m^2 , and the density ρ in unit kg/m^3 , we can find the velocity of wave in the linear elastic media as follows

$$\nu_0 = \sqrt{f'(0)M/\rho}, \quad M := 2 \int_0^1 J(r)rdr.$$

We introduce the time scale $T_0 := L/\nu_0$. Then a wave in the elastic media with elastic constant $C = Mf'(0)$ requires T_0 seconds to reach from one end of the bar to the other end.

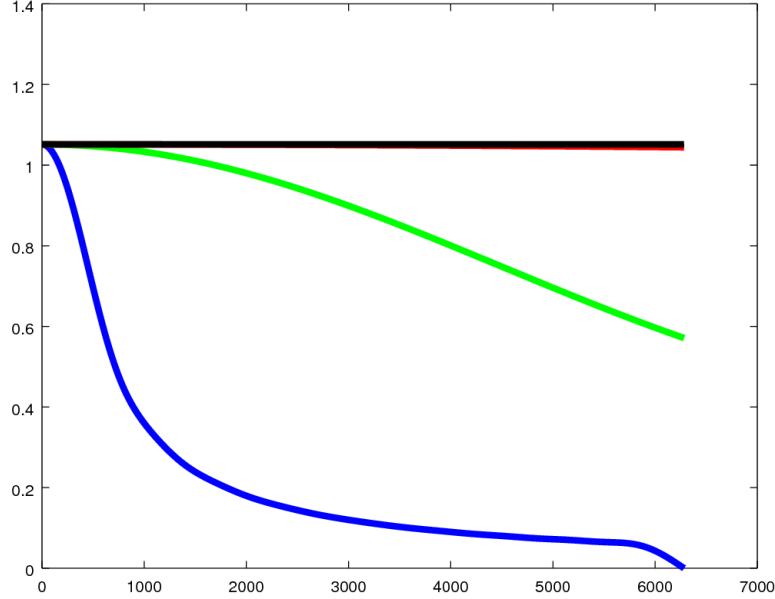


Fig. 4: Normalized phase velocity ν/\sqrt{C} vs wave number κ for different size of horizon. Blue: $\epsilon = 0.01$, Green: $\epsilon = 0.001$, Red: $\epsilon = 0.0001$, Black: $\epsilon = 0.00001$. ϵ/h is fixed to 10. We have fixed κ such that $\kappa \leq 2\pi/h$ for h corresponding to $\epsilon = 0.01$. The influence function is $J(r) = (2/\sqrt{\pi})r \exp[-r^2/0.4]$.

We let $\bar{x} = x/L$ for $x \in [0, L]$, and $\bar{t} = t/T_0$. We define non-dimensional solution $\bar{u}(\bar{x}, \bar{t}) := u(L\bar{x}, T_0\bar{t})/L$. Let $\bar{\epsilon} := \epsilon/L$ be nondimensional size of horizon. Then \bar{u} satisfies

$$\ddot{\bar{u}}(\bar{t}, \bar{x}) = \frac{2}{\bar{\epsilon}^2} \int_{\bar{x}-\bar{\epsilon}}^{\bar{x}+\bar{\epsilon}} \bar{f}'(|\bar{y} - \bar{x}|) \bar{S}(\bar{y}, \bar{x}) J(|\bar{y} - \bar{x}|/\bar{\epsilon}) d\bar{y} + \bar{b}(\bar{t}, \bar{x}),$$

where $\bar{S}(\bar{y}, \bar{x}; \bar{u}(\bar{t})) = (\bar{u}(\bar{t}, \bar{y}) - \bar{u}(\bar{t}, \bar{x}))/|\bar{y} - \bar{x}|$, $\bar{f}'(r) = \frac{L}{C} f'(Lr)$, and $\bar{b}(\bar{t}, \bar{x}) = \frac{L}{C} b(T_0\bar{t}, L\bar{x})$. Given the dimensionless solution \bar{u} of above equation then the solution u for any E , such that $f'(0) = E$, can be obtained from \bar{u} . The time interval T_0 for a given E is given by $T_0 = L\sqrt{\rho/EM}$ and $u(t) = L\bar{u}(t/T_0)$.

In the following studies we choose the influence function to be $J(|x|) = 2|x| \exp(-|x|^2/\alpha)$ with $\alpha = 0.4$. Its dispersion curve is shown in Figure 3 in Red. We define f such that $f'(0) = 1/M$, where $M = 2 \int_0^1 J(r) dr$. This gives $T_0 = 1$. The body force is set to zero, i.e. $b = 0$. All numerical results shown in this article will correspond to above choice of J , b , and f .

6.2. h -convergence. We study the the rate of convergence for two different choices of initial conditions. In first problem, we consider the Gaussian pulse as the initial condition given by: $u_0(x) = a \exp[-(0.5 - x)^2/\beta]$, $v_0(x) = 0.0$ with $a = 0.005$ and $\beta = 0.00001$. The time interval is $[0, 1.7]$ and the time step is $\Delta t = 0.00001$. We fix ϵ to 0.1, and consider the mesh sizes $h = \{\epsilon/10, \epsilon/100, \epsilon/1000\}$. For the second problem, we consider the

Table 1: Convergence result for problem 1. Superscript 1 refers to L^2 norm and 2 refers to sup norm. NPD refers to nonlinear peridynamic and LPD refers to linear peridynamic. Max time step is 170000.

Time step	LPD ¹	NPD ¹	LPD ²	NPD ²
6000	1.6416	1.6419	1.4204	1.4204
51500	1.3098	1.3106	1.3312	1.3331
104000	1.1504	1.1482	1.5155	1.5557
147000	1.1364	1.1262	1.6027	1.5215
165000	1.2611	1.2632	1.5496	1.6055

Table 2: Convergence result for problem 2. Superscript 1 refers to L^2 norm and 2 refers to sup norm. NPD refers to nonlinear peridynamic and LPD refers to linear peridynamic. Max time step is 10^5 .

Time step	LPD ¹	NPD ¹	LPD ²	NPD ²
2000	1.4498	1.4504	1.2546	1.2547
54000	1.3718	1.3707	1.6903	1.6908
96000	1.3735	1.3719	1.3753	1.3816

double Gaussian curve as initial condition: $u_0(x) = a \exp[-(0.25 - x)^2/\beta] + a \exp[-(0.75 - x)^2/\beta]$, $v_0(x) = 0.0$ with $a = 0.005$ and $\beta = 0.00001$. The time interval for the second problem is $[0, 0.5]$ and the time step is $\Delta t = 0.000005$. Here we consider a smaller horizon $\epsilon = 0.01$, and solve for the three mesh sizes $h = \{\epsilon/100, \epsilon/200, \epsilon/400\}$.

Using the approximate solutions corresponding to three different mesh sizes, we can easily compute the dependence of the error with respect to mesh size h . Let u_1, u_2, u_3 correspond to meshes of size h_1, h_2, h_3 , and let u be the exact solution. We write the error as $\|u_h - u\| \leq Ch^\alpha$ for some constant C and $\alpha > 0$, and assuming that the ratio of mesh size is fixed and $h_1/h_2 = h_2/h_3 = r$, we get

$$\begin{aligned} \log(\|u_1 - u_2\|) &\leq C + \alpha \log h_2, \\ \log(\|u_2 - u_3\|) &\leq C + \alpha \log h_3. \end{aligned}$$

Then the rate of convergence α is bounded below by

$$\frac{\log(\|u_1 - u_2\|) - \log(\|u_2 - u_3\|)}{\log(r)}.$$

In [Table 1](#) and [Table 2](#), we list lower bound on the rate of convergence for different times in the evolution. The lower bound on the rate of convergence is seen to depend on the time step. We also note that the bounds on the rate of convergence for the linear peridynamic solution is very close to that of the nonlinear peridynamic solution.

6.3. m -convergence. We consider the limit of peridynamic solution as $\epsilon \rightarrow 0$. Description of problem is as follows: $u_0(x) = a \exp[-(0.5 - x)^2/\beta]$, $v_0(x) = 0.0$ with $a = 0.005$ and $\beta = 0.00001$. Time domain is $[0, 0.1]$ and time step is $\Delta t = 0.0000005$. We fix the ratio $\epsilon/h = 100$, and solve the problem for $\epsilon = \{0.0016, 0.0008, 0.0004\}$. As before we assume a

Table 3: Rate of convergence $\frac{\log(\|u^{\epsilon_1} - u^{\epsilon_2}\|) - \log(\|u^{\epsilon_2} - u^{\epsilon_3}\|)}{\log(\epsilon_2) - \log(\epsilon_3)}$.

Time step	Conv. of LPD		Conv. of NPD	
	L^2	sup	L^2	sup
2000	1.9052	1.5556	1.9052	1.5556
50000	1.7916	1.6275	1.7916	1.6275
100000	1.718	1.449	1.718	1.449
150000	1.6298	1.2688	1.6298	1.2688
200000	1.5388	1.1086	1.5388	1.1086

convergence error $\|u^\epsilon - u\| \leq C\epsilon^\alpha$. The upper bound on the rate is given by

$$\frac{\log(\|u^{\epsilon_1} - u^{\epsilon_2}\|) - \log(\|u^{\epsilon_2} - u^{\epsilon_3}\|)}{\log(\epsilon_2) - \log(\epsilon_3)}.$$

In Table 3, we record the the upper bound on the convergence rate with respect to ϵ for different times in the evolution.

Comparison with the elastodynamic solution: We compare the numerical solutions of elastodynamics, linear peridynamics, and nonlinear peridynamics. The comparison is made using the common initial data given by $u_0(x) = a \exp[-(0.25 - x)^2/\beta] + a \exp[-(0.75 - x)^2/\beta]$, $v_0(x) = 0.0$ with $a = 0.001$ and $\beta = 0.003$. The time interval is $[0, 1.0]$ and the time step is $\Delta t = 0.000001$. Here the time interval is chosen sufficiently large to include the effect of reflection of waves in the boundary. In Figure 5, we plot the error $\|u_{peri} - u_{elasto}\|$ at each time step. Figure 5 validates the fact that error depends on h/ϵ (see Equation 21 and Equation 20). In Figure 6, we plot the solutions at different time steps.

In Figure 5, we see that error increases when t is close to 0.25, 0.5, 0.75, 0.95. The increase near $t = 0.25$ and $t = 0.5$ is due to modeling error and is associated with wave dispersion for the nonlocal models when the wave hits the boundary. This can be seen in the peridynamics simulations with smaller ϵ (compare Green, Cyan, and the Black curves in Figure 5 with that of large ϵ in the Blue, Red, and Yellow curves) and the increase in error near $t = 0.25$ and $t = 0.5$ goes away irrespective of h/ϵ ratio. On the other hand the simulation shows that for times near $t = 0.5, 0.95$, there is interaction between two Gaussian pulses traveling towards each other. This interaction is well captured by peridynamic solutions when ϵ is small along with the finer mesh h chosen so that h/ϵ is small. This fact is seen in the Cyan curve corresponding to smaller ϵ as compared to Blue curve. But the increase near $t = 0.5$ and $t = 0.95$ does not improve much in the Cyan curve. However, this error is greatly reduced in the simulation corresponding to the Black curve where ϵ the same as the Cyan curve but with smaller much smaller h/ϵ .

Comparison between nonlinear and linear peridynamic for smooth solutions: In Proposition 1, we show that difference between the linear and peridynamic force is controlled by ϵ . Therefore, we would expect that as the size of horizon gets smaller the difference between approximate solution of linear and nonlinear peridynamics will get smaller. Let u_l^1, u_l^2 be linear peridynamic solutions and u^1, u^2 be nonlinear peridynamic solutions. The superscript "1" corresponds to $(\epsilon_1 = 0.01, h_1 = \epsilon/50)$ and "2" $(\epsilon_2 = 0.005, h_2 = \epsilon/100)$. The Figure 7 shows the plot of slope $\frac{\log(\|u^1 - u_l^1\|_{L^2}) - \log(\|u^2 - u_l^2\|_{L^2})}{\log(\epsilon_1) - \log(\epsilon_2)}$ at different time steps. We see from the figure that the rate of convergence is very consistent with respect to time and is very close to expected value 1.

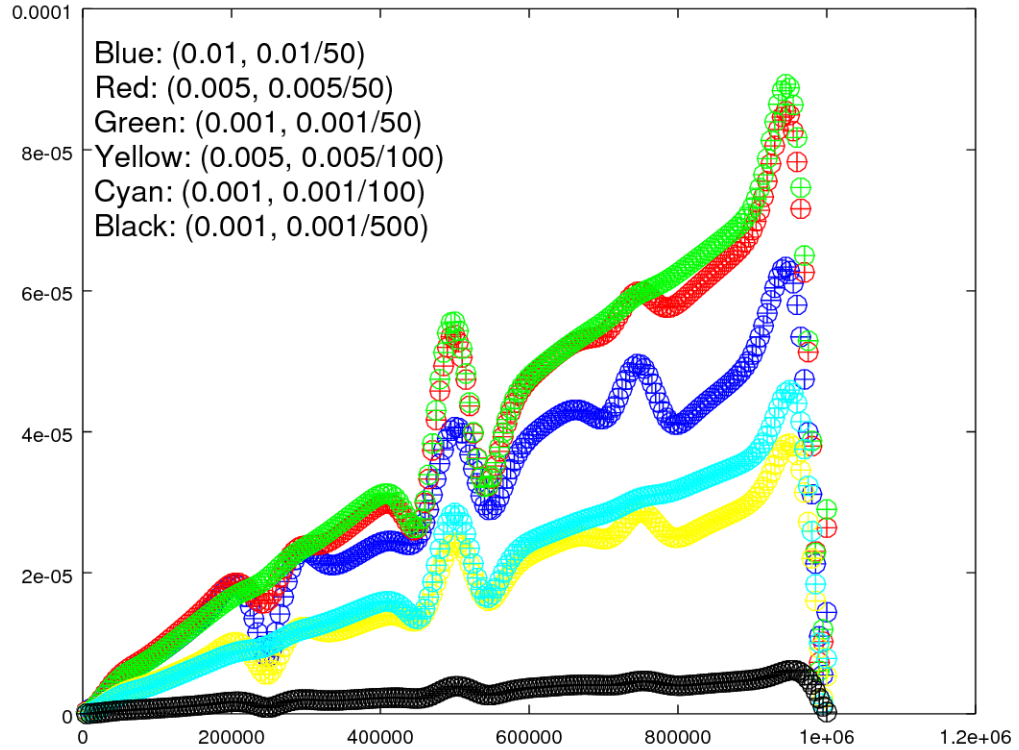


Fig. 5: Plot of $\|u_{peri} - u_{elasto}\|_{L^2}$ at different time steps. Arguments inside the bracket corresponds to (ϵ, h) . “+” corresponds to the linear peridynamics and “o” corresponds to nonlinear peridynamics. For $(\epsilon = 0.005, h = \epsilon/100)$ (Yellow curve), the error $\|u_{peri} - u_{elasto}\|$ is smaller compared to the error for $(\epsilon = 0.01, h = \epsilon/50)$ (Blue curve), whereas for the same $\epsilon = 0.005$ but with $h = \epsilon/50$ (Red curve), error is in fact higher than the error corresponding to $(\epsilon = 0.01, h = \epsilon/50)$ (Blue curve). To further demonstrate the dependence of $\|u_{peri} - u_{elasto}\|$ on h/ϵ , the solution corresponding to $(\epsilon = 0.001, h = \epsilon/100)$ (Cyan curve) lies above the Yellow curve. However, when the ratio ϵ/h is increased to 500 (Black curve), i.e. for $(\epsilon = 0.001, h = \epsilon/500)$, we see that the Black curve is lower than the Yellow curve. Also note that the error plot corresponding to linear and nonlinear peridynamic are almost same (“+” and “o” overlap in each curve).

Combining peridynamic and elastodynamic models: In light of the numerical experiments and theory, we make a case for use of the elastodynamic model in regions where force nonlinearity is not present. The results of this analysis rigorously show that one can use a discrete linear local elastodynamic model to approximate the nonlinear nonlocal evolution when sufficient regularity of the evolution is known a-priori. In doing so one incurs a modeling error of order ϵ but saves computational work in that there is no nonlocality so the mesh diameter h no longer has to be small relative to ϵ . The discretization error is now associated with the approximation error for the initial boundary value problem for the linear

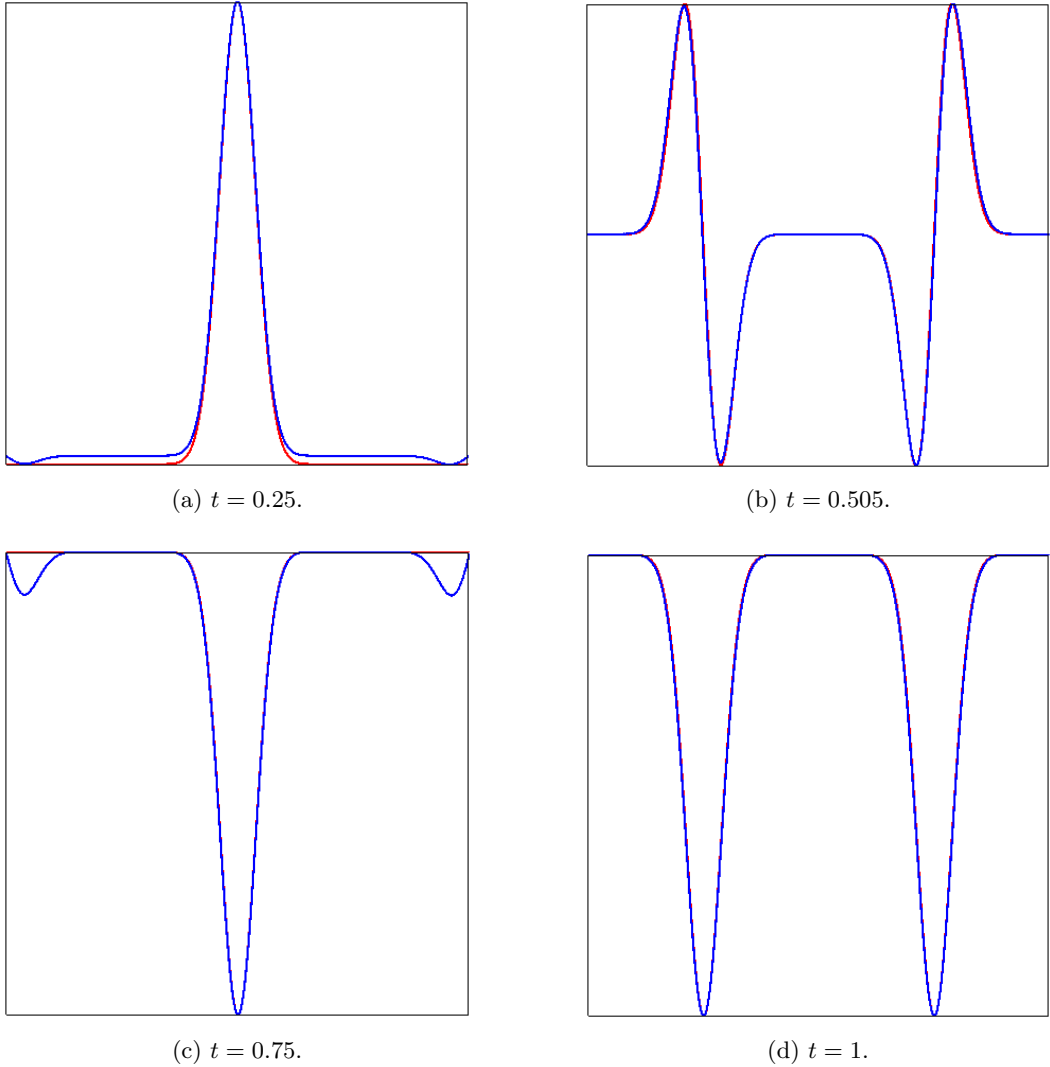


Fig. 6: The elastodynamic solution is shown in Red, linear peridynamics in Green, and nonlinear peridynamics in Blue. Simulation shows that solutions of linear and nonlinear peridynamic are nearly identical. The Green curve is hidden beneath Blue curve. The elastodynamic solution corresponds to mesh size $h = 0.00001$ whereas the peridynamic solution corresponds to $\epsilon = 0.005$ and $h = \epsilon/100$. Plots above are normalized so that the displacement lies within $[0, 1]$.

elastic wave equation. Earlier theoretical work shows that this model delivers evolutions asymptotically close to sharp discontinuities with bounded Griffiths fracture energy as ϵ goes to zero, as well as evolutions that solve local elastodynamics away from the crack set [22], [23], [21]. The investigation carried out here shows that evolutions are numerically well approximated by linear elastodynamics in regions where strains are regular and ϵ is small.

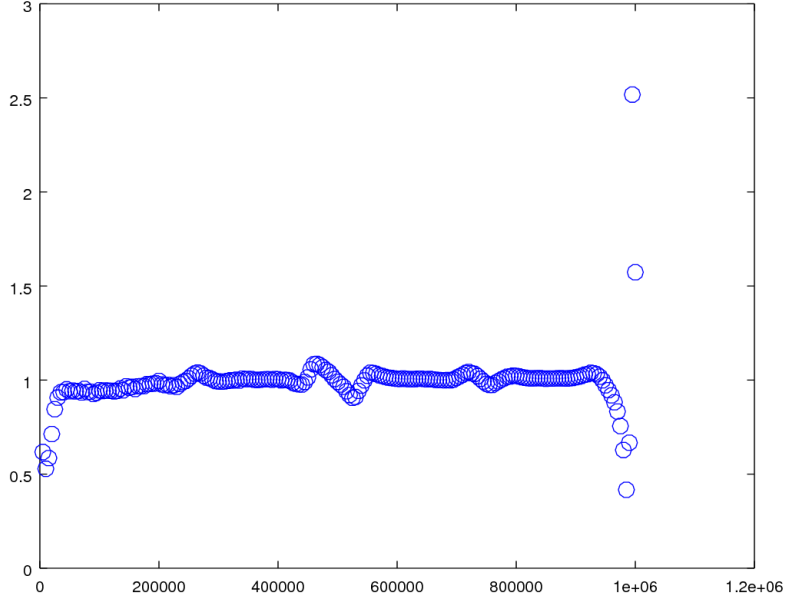


Fig. 7: Slope of $\log(\|u_{NPD} - u_{LPD}\|_{L^2})$ with respect to $\log(\epsilon)$ at different time steps from $k = 0$ to $k = 10^6$.

7. Proof of claims. In this section, we will present the proof of claims in section 2 and section 3. For simplification, we adopt the following notation

$$(25) \quad \begin{aligned} p &:= u_x(x), & q &:= u_{xx}(x), & r &:= u_{xxx}(x), \\ e &:= \frac{(y-x)}{|y-x|} = \text{sign}\{y-x\}. \end{aligned}$$

In proving results related to consistency error, we will employ the Taylor series expansion of $u(y)$ with respect to point x_i . Since the potential f is assumed to be sufficiently smooth, $f''(r)$, $f'''(r)$, and $f''''(r)$ are bounded for $0 < r < \infty$.

7.1. Bound on difference of peridynamic, linear peridynamic, and elastodynamic force. We prove [Proposition 1](#) for $u \in C^3(D)$. Using Taylor series expansion, we get

$$\begin{aligned} S(y, x; u) &= u_x(x) \frac{y-x}{|y-x|} + 1/2 u_{xx}(x) |y-x| + 1/6 u_{xxx}(\xi) |y-x| (y-x) \\ &= pe + q|y-x|/2 + T_1(y-x)/|y-x|, \end{aligned}$$

where $T_1 = O(|y-x|^3)$. On taking the Taylor series expansion of the nonlinear potential, and substituting in the expansion above, we get

$$\begin{aligned} & (f'(|y-x|S(y, x; u)^2) - f'(0)) S(y, x; u) \\ &= f''(0)p^3|y-x|e + (f''(0)p^2q3/2 + f'''(0)p^5e/2)|y-x|^2 + T_2(y-x), \end{aligned}$$

where $T_2(y - x) = O(|y - x|^3)$. Using the previous equation, we get

$$\begin{aligned}
& -\nabla PD^\epsilon_l(u)(x) + \nabla PD_l^\epsilon(u)(x) \\
&= \frac{2}{\epsilon^2} \int_{x-\epsilon}^{x+\epsilon} J(|y - x|/\epsilon) (f'(|y - x|S(y, x; u)^2) - f'(0)) S(y, x; u) dy \\
&= \frac{2}{\epsilon^2} \int_{x-\epsilon}^{x+\epsilon} [f''(0)p^3|y - x|e \\
&\quad + (f''(0)p^2q3/2 + f'''(0)p^5e/2)|y - x|^2 + T_2(y - x)] J(|y - x|/\epsilon) dy \\
&= \frac{2}{\epsilon^2} \int_{x-\epsilon}^{x+\epsilon} f''(0)p^2q3/2|y - x|^2 J(|y - x|/\epsilon) dy + O(\epsilon^2) \\
&= O(\epsilon),
\end{aligned}$$

where terms with e integrate to zero. From this, we see that same estimate holds when u has continuous and bounded third or fourth derivatives. This proves the assertion of [Proposition 1](#).

To prove [Equation 7](#), we proceed as follows

$$\begin{aligned}
-\nabla PD_l^\epsilon(u)(x) &= \frac{2}{\epsilon^2} \int_{x-\epsilon}^{x+\epsilon} J(|y - x|/\epsilon) f'(0) S(y, x; u) dy \\
&= \frac{2}{\epsilon^2} \int_{x-\epsilon}^{x+\epsilon} J(|y - x|/\epsilon) f'(0) [pe + q|y - x|/2 + T_1(y - x)/|y - x|] dy \\
&= \left(\frac{2}{\epsilon^2} \int_{x-\epsilon}^{x+\epsilon} J(|y - x|/\epsilon) f'(0) |y - x|/2 dy \right) q + O(\epsilon) \\
&= \mathbb{C}u_{xx}(x) + O(\epsilon),
\end{aligned}$$

where we identify \mathbb{C} using [Equation 2](#), and $q = u_{xx}(x)$. This proves [Equation 7](#).

To prove [Equation 10](#), we assume $u \in C^4(D)$ and [Equation 9](#). Then, by Taylor series expansion, we have

$$\begin{aligned}
S(y, x; u) &= u_x(x) \frac{y - x}{|y - x|} + 1/2u_{xx}(x)|y - x| \\
&\quad + 1/6u_{xxx}(x)|y - x|(y - x) + 1/24u_{xxxx}(\xi)|y - x|^3 \\
&= pe + q|y - x|/2 + r|y - x|^2e + T_1(y - x)/|y - x|,
\end{aligned}$$

where $T_1(y - x) = O(|y - x|^4)$. Substituting this into $-\nabla PD_l^\epsilon(u)(x)$, and noting that terms with e integrate to zero, we get

$$-\nabla PD_l^\epsilon(u)(x) = \mathbb{C}u_{xx}(x) + O(\epsilon^2).$$

7.2. Convergence of solution of peridynamic equation to the elastodynamic equation. To prove [Theorem 2](#), we proceed as follows. Let u^ϵ be the solution of peridynamic model in [Equation 4](#), and let u be the solution of elastodynamic equation in [Equation 3](#). Boundary conditions and initial conditions are same as described in [section 2](#). Assuming that the hypothesis of [Theorem 2](#) holds, we have from [Proposition 1](#)

$$-\nabla PD^\epsilon(u^\epsilon(t))(x) = \mathbb{C}u_{xx}^\epsilon(t, x) + O(\epsilon).$$

We have also assumed that there exists $C_1 < \infty$ such that

$$\sup_{\epsilon > 0} \left[\sup_{(x, t) \in D \times J} |u_{xxxx}^\epsilon(t, x)| \right] < C_1 < \infty.$$

Combining this together with [Equation 8](#) we have,

$$\sup_{(x,t) \in D \times J} | -\nabla P D^\epsilon(u^\epsilon(t))(x) - \mathbb{C} u_{xx}^\epsilon(t, x) | \leq C_3 \epsilon,$$

where C_3 is independent of x, t and ϵ . Subtracting equation [Equation 4](#) from equation [Equation 3](#) shows that $e^\epsilon = u^\epsilon - u$ satisfies

$$\begin{aligned} \rho \ddot{e}^\epsilon(t, x) &= \mathbb{C} e_{xx}^\epsilon(t, x) + (-\nabla P D^\epsilon(u^\epsilon(t))(x) - \mathbb{C} u_{xx}^\epsilon(t, x)) \\ (26) \quad &= \mathbb{C} e_{xx}^\epsilon(t, x) + F(t, x), \end{aligned}$$

where

$$F(t, x) = -\nabla P D^\epsilon(u^\epsilon(t))(x) - \mathbb{C} u_{xx}^\epsilon(t, x) \quad \text{and} \quad \sup_{(x,t) \in D \times J} |F(t, x)| \leq C_3 \epsilon,$$

with boundary condition and initial condition given by

$$\begin{aligned} e^\epsilon(0, x) &= 0, & \dot{e}^\epsilon(0, x) &= 0 & \forall x \in D, \\ e^\epsilon(t, x) &= 0, & \dot{e}^\epsilon(t, x) &= 0 & \forall (t, x) \in [0, T] \times \partial D^\epsilon. \end{aligned}$$

Since e^ϵ satisfies [Equation 26](#) we can apply Gronwall's inequality to find

$$(27) \quad \sup_{t \in J} \int_D \rho |\dot{e}^\epsilon(t, x)|^2 dx + \int_D \mathbb{C} |e_x^\epsilon(t, x)|^2 dx \leq C_2 \epsilon^2.$$

Now to show that $e^\epsilon \rightarrow 0$ in $H^1(D)$, we apply [Equation 27](#) together with Poincare's inequality to get

$$\begin{aligned} \|e^\epsilon(t, x)\|_{L^2(D)}^2 &\leq C \|e_x^\epsilon(t, x)\|_{L^2(D)}^2 \\ &\leq \frac{C}{\mathbb{C}} \sup_{t \in [0, T]} \left\{ \int_D \rho |\dot{e}^\epsilon(t, x)|^2 dx + \int_D \mathbb{C} |e_x^\epsilon(t, x)|^2 dx \right\} \\ &\leq \frac{C}{\mathbb{C}} C_2 \epsilon^2, \end{aligned}$$

where C is the Poincare constant. On collecting results this shows that $e^\epsilon \rightarrow 0$ in the $H^1(D)$ norm with the rate ϵ . This completes the proof of [Theorem 2](#). Identical arguments using [Equation 10](#) deliver [Theorem 3](#).

7.3. Bounds on the consistency error. In this section [Proposition 4](#) is established. We begin by writing the difference $S(y, x_i; \mathcal{I}_h[u]) - S(y, x_i; u)$. It is given by

$$S(y, x_i; \mathcal{I}_h[u]) - S(y, x_i; u) = \frac{\mathcal{I}_h[u](y) - u(y)}{|y - x_i|}.$$

From the hypothesis of [Proposition 4](#) there is a constant C for which $|u_{xx}| < C$ on D . Using the approximation property $|\mathcal{I}_h[u] - u| \leq Ch^2$ and applying $|y - x_i| > h$ for y outside the interval $[x_{i-1}, x_{i+1}]$ gives

$$|S(y, x_i; \mathcal{I}_h[u]) - S(y, x_i; u)| \leq \begin{cases} C|y - x_i| & \text{if } y \in [x_{i-1}, x_{i+1}], \\ Ch & \text{if } y \in [x_i - \epsilon, x_{i-1}], \\ Ch & \text{if } y \in [x_{i+1}, x_i + \epsilon]. \end{cases}$$

Note further that $|y - x_i| \leq h$ for $y \in [x_{i-1}, x_{i+1}]$ and we conclude

$$(28) \quad |S(y, x_i; \mathcal{I}_h[u]) - S(y, x_i; u)| \leq Ch.$$

Straight forward calculation shows

$$\begin{aligned} |\nabla PD_\ell^\epsilon(\mathcal{I}_h[u]) - \nabla PD_\ell^\epsilon(u)| &\leq \frac{2f'(0)}{\epsilon^2} \int_{x_i-\epsilon}^{x_i+\epsilon} |S(y, x_i; \mathcal{I}_h[u]) - S(y, x_i; u)| J(|y - x_i|/\epsilon) dy \\ &\leq \frac{4f'(0)MC\epsilon}{\epsilon}, \end{aligned}$$

where $M = \max_{0 \leq z < 1} J(z)$ and [Equation 18 of Proposition 4](#) follows.

We now establish the consistency error for the nonlinear nonlocal model. We begin with an estimate for the strain. Applying the notation described in [Equation 25](#) with p and e defined for $x = x_i$ we apply Taylor's theorem with remainder to get

$$(29) \quad \begin{aligned} S(y, x_i; u) &= u_x(x_i)(y - x_i)/|y - x_i| + u_{xx}(\xi)|y - x_i|/2 \\ &= pe + T_1(y - x_i)/|y - x_i| \end{aligned}$$

where $T_1(y - x_i) = O(|y - x_i|^2)$.

From [Equation 28](#) we can write

$$S(y, x_i; u) = S(y, x_i; \mathcal{I}_h[u]) + O(h),$$

or

$$(30) \quad S(y, x_i; \mathcal{I}_h[u]) = S(y, x_i; u) + O(h),$$

or we can write $S(y, x_i; u) = S(y, x_i; \mathcal{I}_h[u]) + \eta$, where $|\eta| < Ch$. Adopting this convention first we write

$$\begin{aligned} |y - x_i|S^2(y, x_i; u) &= |y - x_i|(S(y, x_i; \mathcal{I}_h[u]) + \eta)^2 \\ &= |y - x_i|S^2(y, x_i; \mathcal{I}_h[u]) + \sum_{j \in I} 2\eta\phi_j(y)(u(x_j) - u(x_i)) + |y - x_i|\eta^2, \end{aligned}$$

where the set $I = \{j : x_j \in [x_i - \epsilon, x_i + \epsilon]\}$ and we have used the identity

$$1 = \sum_{j \in I} \phi_j(y), \quad y \in [x_i - \epsilon, x_i + \epsilon].$$

Next we estimate

$$\begin{aligned} \sum_{j \in I} \phi_j(y)(u(x_j) - u(x_i)) &\leq \sup\{|u(y) - u(x_i)| \text{ for } y \in [x_i - \epsilon, x_i + \epsilon]\} \\ &\leq 2\epsilon \sup_{y \in D} |u_x(y)|. \end{aligned}$$

Since u_x is bounded we see that $\sum_{j \in I} \phi_j(y)(u(x_j) - u(x_i)) = \zeta$ where $|\zeta| \leq \epsilon \text{Const.}$ and

$$|y - x_i|S^2(y, x_i; u) = |y - x_i|(S(y, x_i; \mathcal{I}_h[u]))^2 + 2\zeta\eta + \eta^2$$

Applying Taylor's theorem with remainder to the function $f'(|y - x|(S(y, x_i; \mathcal{I}_h[u]) + \eta)^2)$ now gives

$$(31) \quad f'(|y - x|S(y, x_i; u)^2) = f'(|y - x|(S(y, x_i; \mathcal{I}_h[u]))^2) + O(h),$$

where we have used that $f''(r)$ is bounded on $0 \leq r \leq \infty$.

Then application of Equation 29, Equation 30, and Equation 31 and substitution delivers the desired estimate

$$\begin{aligned} & -\nabla PD^\epsilon(\mathcal{I}_h[u])(x_i) + \nabla PD^\epsilon(u)(x_i) \\ &= \frac{2}{\epsilon^2} \int_{x_i-\epsilon}^{x_i+\epsilon} f'(|y - x|(S(y, x_i; \mathcal{I}_h[u]))^2) (S(y, x_i; u) + O(h)) J(|y - x_i|/\epsilon) dy - \\ & - \frac{2}{\epsilon^2} \int_{x_i-\epsilon}^{x_i+\epsilon} (f'(|y - x|(S(y, x_i; \mathcal{I}_h[u]))^2) + O(h)) S(y, x_i; u) J(|y - x_i|/\epsilon) dy \\ &= O(h/\epsilon), \end{aligned}$$

and Equation 19 of Proposition 4 is proved.

8. Conclusion. Earlier work [21] analyzed the same model but for more general initial data that generated non differentiable Hölder continuous solutions. For that case solutions can approach discontinuous deformations (fracture like solutions) as $\epsilon \rightarrow 0$ and it is shown that the numerical approximation of the nonlinear model in dimension $d = 1, 2, 3$ converges to the exact solution at the rate $O(\Delta t + h^\gamma/\epsilon^2)$ where $\gamma \in (0, 1]$ is the Hölder exponent, h is the size of mesh, ϵ is the size of horizon, and Δt is the size of time step. Here we have shown that we can improve the rate of convergence if we somehow have a-priori knowledge on the number of bounded continuous derivatives of the solution.

From the perspective of computation, the resolution of the mesh inside the horizon of nonlocal interaction is the main contributor to the computational complexity. This work provides explicit error estimates for the differences between the solutions of elastodynamics and nonlocal models. It shows that the effects of the mesh size relative to the horizon become significant. Numerical errors can grow with decreasing horizon if the mesh is not chosen suitably small with respect to the peridynamic horizon. A fixed ratio of mesh size to horizon will not increase accuracy as the horizon tends to zero. We have carried out numerical simulations where the accuracy decreases when ϵ is reduced and the ratio h/ϵ is fixed. This is in line with the consistency error bounds that vanish at the rate $O(h/\epsilon)$.

REFERENCES

- [1] Robert J. Plemmons Abraham Berman. *Nonnegative matrices in the mathematical sciences*. Classics in applied mathematics 9. Society for Industrial and Applied Mathematics, 1987.
- [2] Abigail Agwai, Ibrahim Guven, and Erdogan Madenci. Predicting crack propagation with peridynamics: a comparative study. *International journal of fracture*, 171(1):65–78, 2011.
- [3] B. Aksyulu and Z. Unlu. Conditioning analysis of nonlocal integral operators in fractional sobolev spaces. *SIAM Journal on Numerical Analysis*, 52:653–677, 2014.
- [4] Burak Aksyulu and Michael L Parks. Variational theory and domain decomposition for nonlocal problems. *Applied Mathematics and Computation*, 217(14):6498–6515, 2011.
- [5] Zdeněk P Bažant, Wen Luo, Viet T Chau, and Miguel A Bessa. Wave dispersion and basic concepts of peridynamics compared to classical nonlocal damage models. *Journal of Applied Mechanics*, 83(11):111004, 2016.
- [6] Florin Bobaru and Wenke Hu. The meaning, selection, and use of the peridynamic horizon and its relation to crack branching in brittle materials. *International journal of fracture*, 176(2):215–222, 2012.

- [7] Florin Bobaru, Mijia Yang, Leonardo Frota Alves, Stewart A Silling, Ebrahim Askari, and Jifeng Xu. Convergence, adaptive refinement, and scaling in 1d peridynamics. *International Journal for Numerical Methods in Engineering*, 77(6):852–877, 2009.
- [8] Xi Chen and Max Gunzburger. Continuous and discontinuous finite element methods for a peridynamics model of mechanics. *Computer Methods in Applied Mechanics and Engineering*, 200(9):1237–1250, 2011.
- [9] Kaushik Dayal. Leading-order nonlocal kinetic energy in peridynamics for consistent energetics and wave dispersion. *Journal of the Mechanics and Physics of Solids*, 105:235–253, 2017.
- [10] Kaushik Dayal and Kaushik Bhattacharya. Kinetics of phase transformations in the peridynamic formulation of continuum mechanics. *Journal of the Mechanics and Physics of Solids*, 54(9):1811–1842, 2006.
- [11] P Diehl, R Lipton, and MA Schiweitzer. Numerical verification of a bond-based softening peridynamic model for small displacements: Deducing material parameters from classical linear theory. 2016.
- [12] Qiang Du, Max Gunzburger, Richard B Lehoucq, and Kun Zhou. Analysis and approximation of nonlocal diffusion problems with volume constraints. *SIAM review*, 54(4):667–696, 2012.
- [13] Qiang Du and Kun Zhou. Mathematical analysis for the peridynamic nonlocal continuum theory. *ESAIM: Mathematical Modelling and Numerical Analysis*, 45(2):217–234, 2011.
- [14] Etienne Emmrich, Richard B Lehoucq, and Dimitri Puhst. Peridynamics: a nonlocal continuum theory. In *Meshfree Methods for Partial Differential Equations VI*, pages 45–65. Springer, 2013.
- [15] Bobaru Florin, John T Foster, Philippe H Geubelle, Philippe H Geubelle, and Stewart A Silling. Handbook of peridynamic modeling, 2016.
- [16] John T Foster, Stewart A Silling, and Weinong Chen. An energy based failure criterion for use with peridynamic states. *International Journal for Multiscale Computational Engineering*, 9(6), 2011.
- [17] M Ghajari, L Iannucci, and P Curtis. A peridynamic material model for the analysis of dynamic crack propagation in orthotropic media. *Computer Methods in Applied Mechanics and Engineering*, 276:431–452, 2014.
- [18] Qingguang Guan and Max Gunzburger. Stability and accuracy of time-stepping schemes and dispersion relations for a nonlocal wave equation. *Numerical Methods for Partial Differential Equations*, 31(2):500–516, 2015.
- [19] Youn Doh Ha and Florin Bobaru. Studies of dynamic crack propagation and crack branching with peridynamics. *International Journal of Fracture*, 162(1-2):229–244, 2010.
- [20] Youn Doh Ha and Florin Bobaru. Characteristics of dynamic brittle fracture captured with peridynamics. *Engineering Fracture Mechanics*, 78(6):1156–1168, 2011.
- [21] Prashant K Jha and Robert Lipton. Numerical analysis of peridynamic models in $h\backslash$ older space. *arXiv preprint arXiv:1701.02818*, 2017.
- [22] Robert Lipton. Dynamic brittle fracture as a small horizon limit of peridynamics. *Journal of Elasticity*, 117(1):21–50, 2014.
- [23] Robert Lipton. Cohesive dynamics and brittle fracture. *Journal of Elasticity*, 2015.
- [24] Robert Lipton, Stewart Silling, and Richard Lehoucq. Complex fracture nucleation and evolution with nonlocal elastodynamics. *arXiv preprint arXiv:1602.00247*, 2016.
- [25] Tadele Mengesha and Qiang Du. Analysis of a scalar peridynamic model with a sign changing kernel. *Discrete Contin. Dynam. Systems B*, 18:1415–1437, 2013.
- [26] Tadele Mengesha and Qiang Du. Nonlocal constrained value problems for a linear peridynamic navier equation. *Journal of Elasticity*, 116(1):27–51, 2014.
- [27] SA Silling, O Weckner, E Askari, and Florin Bobaru. Crack nucleation in a peridynamic solid. *International Journal of Fracture*, 162(1-2):219–227, 2010.
- [28] Stewart A Silling. Reformulation of elasticity theory for discontinuities and long-range forces. *Journal of the Mechanics and Physics of Solids*, 48(1):175–209, 2000.
- [29] Stewart A Silling and Ebrahim Askari. A meshfree method based on the peridynamic model of solid mechanics. *Computers & structures*, 83(17):1526–1535, 2005.
- [30] Stewart A Silling and Richard B Lehoucq. Convergence of peridynamics to classical elasticity theory. *Journal of Elasticity*, 93(1):13–37, 2008.
- [31] Stewart Andrew Silling and Florin Bobaru. Peridynamic modeling of membranes and fibers. *International Journal of Non-Linear Mechanics*, 40(2):395–409, 2005.
- [32] X. Tian and Q. Du. Asymptotically compatible schemes and applications to robust discretization of nonlocal models. *SIAM Journal on Numerical Analysis*, 52(4):1641–1665, 2014.
- [33] Xiaochuan Tian, Qiang Du, and Max Gunzburger. Asymptotically compatible schemes for the approximation of fractional laplacian and related nonlocal diffusion problems on bounded domains. *Advances in Computational Mathematics*, 42(6):1363–1380, 2016.
- [34] Xiaochuan Tian, Qiang Du, and Max Gunzburger. Asymptotically compatible schemes for the approximation of fractional laplacian and related nonlocal diffusion problems on bounded domains. *Advances in Computational Mathematics*, 42(6):1363–1380, 2016.

- [35] Olaf Weckner and Rohan Abeyaratne. The effect of long-range forces on the dynamics of a bar. *Journal of the Mechanics and Physics of Solids*, 53(3):705–728, 2005.
- [36] Olaf Weckner, Gerd Brunk, Michael A Epton, Stewart A Silling, and Ebrahim Askari. Comparison between local elasticity and non-local peridynamics. *Sandia National Laboratory Report J*, 1109:2009, 2009.
- [37] Olaf Weckner and Etienne Emmrich. Numerical simulation of the dynamics of a nonlocal, inhomogeneous, infinite bar. *J. Comput. Appl. Mech*, 6(2):311–319, 2005.
- [38] Olaf Weckner, Stewart Silling, and Abe Askari. Dispersive wave propagation in the nonlocal peridynamic theory. In *ASME 2008 International Mechanical Engineering Congress and Exposition*, pages 503–504. American Society of Mechanical Engineers, 2008.
- [39] Raymond A Wildman and George A Gazonas. A finite difference-augmented peridynamics method for reducing wave dispersion. *International Journal of Fracture*, 190(1-2):39–52, 2014.